

## New Measurements of $G$ Using the Measurement Standards Laboratory Torsion Balance

T. R. Armstrong\* and M. P. Fitzgerald

*Measurement Standard Laboratory of New Zealand, Industrial Research, P.O. Box 31-310 Lower Hutt, New Zealand*  
(Received 12 May 2003; published 13 November 2003)

This Letter presents the results of a series of measurements of the Newtonian gravitational constant  $G$  using the compensated torsion balance developed at the Measurement Standards Laboratory. Since our last published result using the torsion balance in the compensated mode of operation [Meas. Sci. Technol. **10**, 439 (1999)], several improvements have been made to reduce the uncertainty in the final result. The new measurements have used both stainless steel and copper large masses. The values of  $G$  for the two sets of masses are in good agreement. After combining all of the measurements we get a value of  $G = 6.673\,87(0.000\,27) \times 10^{-11} \text{ m}^3 \text{ kg}^{-1} \text{ s}^{-2}$ . This new value is 5 parts in  $10^5$  smaller than our previous published values.

DOI: 10.1103/PhysRevLett.91.201101

PACS numbers: 04.80.Cc, 06.20.Jr

In 1998 the CODATA committee decided to increase the uncertainty in the recommended value for the Newtonian gravitational constant  $G$  by about 12 times to 1.5 parts in  $10^{-3}$  [1]. Since then a number of new measurements of  $G$  have been completed with three of them having uncertainties below 5 parts in  $10^5$ . The measurements of Gundlach and Merkowitz [2] and Schlamminger *et al.* [3] are in good agreement with each other while the result of Quinn *et al.* [4] is 2 parts in  $10^4$  higher.

We have been making precise measurements of  $G$  using the Measurement Standard Laboratory (MSL) torsion balance for over ten years [5–8]. Over that time, we have improved the apparatus, the measurement method, and the analysis of the results. The results of our final measurement of  $G$  are described in this Letter.

Figure 1 shows a schematic diagram of our torsion balance. It uses two large cylindrical masses ( $\sim 27$  kg each) to produce a gravitational attraction on a  $\sim 500$  g cylindrical small mass made of copper. The small mass is suspended from a  $\sim 1$  m long tungsten fiber with a rectangular cross section of  $300 \mu\text{m} \times 17 \mu\text{m}$  so that it is free to rotate in response to the gravitational attraction of the large masses. This rotation is detected by an autocollimator viewing a mirror attached to the small mass. The signal from the autocollimator goes to a feedback control system to generate a voltage applied to an electrometer. This produces an electrostatic force on the small mass that compensates the gravitational attraction so that the fiber is not required to twist. At each large mass position, positive and negative voltages are used to permit the calculation of the contact potential  $V_c$  between the stainless steel of the electrometer plates and the copper small mass.

The electrometer consists of the four plates below and four plates above the small mass connected as two diagonally opposite pairs of electrodes. The lower four plates are shown in Fig. 1 and four similar plates are positioned above the small mass. The box surrounding the elec-

trometer is earthed. The small mass is also earthed and acts as the moving vane of the electrometer. The electrometer can produce a torque on the small mass in either the clockwise or the anticlockwise direction by applying a voltage to the appropriate pairs of electrodes.

The large masses are kinematically mounted on a turntable that rotates them about the small mass system stopping at the two angular positions corresponding to the maximum in the gravitationally induced torque on the small mass. At each large mass position, the voltage  $V_G$  required to hold the small mass at the same constant position is measured and  $G$  is determined from

$$G(K_I - K_{II}) = 0.5[(dC/d\theta)_1(V_{G_I} + V_c)^2 - (dC/d\theta)_2(V_{G_{II}} + V_c)^2] \quad (1)$$

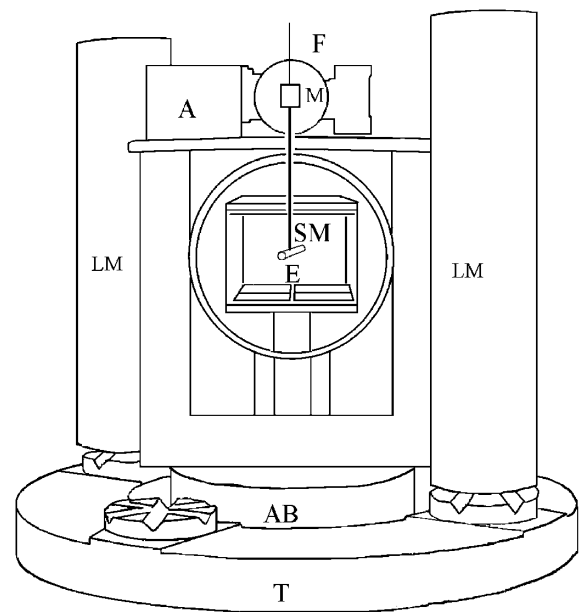


FIG. 1. A schematic diagram of the MSL torsion balance. SM, small mass; LM, large masses; T, turntable; A, autocollimator; F, fiber; AB, air bearing; E, electrometer; M, mirror.

where the subscripts I and II refer to the large mass positions at the maximum of the gravitationally induced torque on either side of the small mass and the subscripts 1 and 2 refer to the two pairs of electrometer electrodes.  $dC/d\theta$  is the change in the electrometer capacitance with angular position of the small mass system.  $K$  is the numerically calculated torque divided by  $G$ .  $K$  depends on the length, mass, and position measurements of the small and large masses and is calculated by a volume integration over the masses using Heyl's [9] formula for the gravitational attraction of a finite cylinder to any external point. An important component of  $K$  is the distance between the large masses. This spacing is measured every time the masses are loaded onto the apparatus by comparison with a calibrated length bar using a specially designed comparator [10].

$V_c$  is determined from

$$V_c = \Delta\Gamma_i / [(dC/d\theta)_i (V_{G+} - V_{G-})] - 0.5(V_{G+} + V_{G-}), \quad (2)$$

where  $V_{G+}$  and  $V_{G-}$  are the values of  $V_G$  measured with positive and negative voltages, respectively.  $\Delta\Gamma_i$  is the difference in the residual torque due to a twist in the fiber between the measurements of  $V_{G+}$  and  $V_{G-}$  and the subscript  $i$  refers to the pair of electrometer electrodes used.

$dC/d\theta$  for each side of the electrometer is determined in a separate measurement. The large masses are removed and a voltage  $V_A$  is applied to one pair of electrodes. This produces a torque that accelerates the small mass towards the electrodes on which  $V_A$  is applied. The signal from the autocollimator is fed to a control loop that changes the angular position of the apparatus. The whole upper part of the apparatus is mounted on an air bearing with a motor drive to allow the apparatus to rotate. The net result is that the apparatus accelerates at the same rate as the small mass to ensure that the fiber does not twist. The angular position of the apparatus is determined by a second autocollimator viewing a polygon attached to the apparatus below the air bearing. The  $dC/d\theta$  values are calculated using

$$dC/d\theta_i = 2(I\alpha_i - \Gamma_R)/(V_A + V_{ci})^2, \quad (3)$$

where  $I$  is the moment of inertia of the small mass system (including the mirror and other small components),  $\alpha$  is the angular acceleration of the apparatus, and  $\Gamma_R$  is the net change in the gravitationally induced torque seen by the apparatus as it rotates through the laboratory. Because the apparatus is accelerating the net effect over a  $2\pi$  rad rotation is not zero. This term also includes the torque produced by any residual twist in the fiber at the time of the acceleration measurement. The two large masses containing  $\sim 100$  kg of lead shot used in the previous measurement [6] to minimize the effect of the local gravitational gradient due to a nearby hill were also used in the current measurements.

When the results from the two parts of the measurement are combined,  $G$  depends upon the ratio  $I/K$ . This means that, although both  $I$  and  $K$  depend strongly upon the length, mass, and density uniformity of the small mass, the ratio does not because of similar terms in the two calculations. This is a significant advantage of using the acceleration method to measure  $dC/d\theta$  in a compensated measurement as the density uniformity of the small mass is a difficult quantity to measure to the required precision. A similar ratio occurs in torsion balances used in the oscillating mode.

Further details about our method and apparatus can be found in [5–8,10].

The main changes made to the torsion balance since the last compensated measurements are that the vacuum system is now remotely mounted to allow continuous pumping when measuring the gravitational signal, a magnetic damper has been added to the torsion balance to damp out the pendulum modes of oscillation (see [8] for further details), and large copper masses have been used as well as the stainless steel attracting masses used in the earlier measurements.

We have also altered a number of features of the measurement of  $dC/d\theta$ . One measurement of the two  $dC/d\theta$  terms uses three to six voltages in the range 30–270 V. We then use Eq. (3), in conjunction with the  $V_c$  terms determined in the gravitational torque measurements, to fit for the two  $dC/d\theta$  terms and  $\Gamma_R$ . Previously, we determined  $\Gamma_R$  in a separate experiment by measuring it at a number of angular positions in the laboratory before each series of acceleration measurements.

To simplify the calculation of the final uncertainty, we have changed the measurement procedure. A measurement of  $G$  is now as follows: (i) measure the angle  $\phi_{FM}$  where the gravitationally induced torque is a maximum; (ii) measure the large mass spacing; (iii) measure  $V_G$  for either one or two weeks (the data from three successive 80 min measurements of  $V_G$  are combined to produce one value of  $G$ ); (iv) measure the large mass spacing; (v) measure  $dC/d\theta$  for three days; (vi) rotate the masses either about their axis or move them to the alternative position on the turntable and repeat steps (ii)–(vi) until all combinations of positions have been used; (vii) re-measure  $\phi_{FM}$ .

The advantage of the new measurement procedure is that we can analyze the data as one complete measurement of  $G$  and most of the uncertainty components are included in the type  $A$  uncertainty of the  $G$  values. The values of  $V_c$  required to determine  $dC/d\theta$  are calculated by fitting the surrounding  $V_G$  measurements and, in the same way, the surrounding  $dC/d\theta$  values are interpolated when calculating  $V_G$  measurements. As the procedure is iterative, we reanalyze the data several times until the final result changes by less than 1 part in  $10^{-6}$ . In previous measurements we analyzed the results by treating the measurements of  $V_G$  and  $dC/d\theta$  as separate

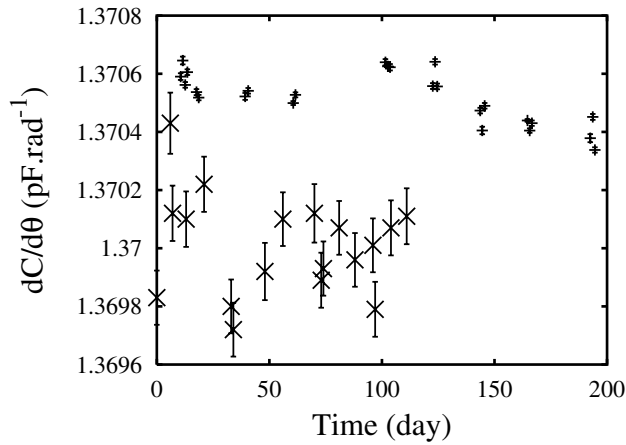


FIG. 2. The measured values of  $dC/d\theta$  for one side of the electrometer for one of the recent measurements of  $G$  plotted with '+'s. Also shown are the values for the same side of the electrometer measured during the 1999 measurement of  $G$  (indicated by 'x's).

experiments. This meant that one common  $dC/d\theta$  value was used to calculate  $G$  so that it was a type  $B$  uncertainty in the final result.

The results of the calibration of one side of the electrometer are shown in Fig. 2 as a function of time for one complete measurement of  $G$ . Overlaid on the graph are the values for the same side of the electrometer from the 1999 measurement of  $G$ . The significant reduction in the variation of the results in the latest series of measurements can be clearly seen. The reduction is due to the improved method of determining the  $\Gamma_R$  term in Eq. (3). The standard uncertainty of the  $dC/d\theta$  values shown in Fig. 2 is 13 ppm for the latest set of measurements, while for the earlier measurements the uncertainty is 30 ppm.

The new  $dC/d\theta$  measurements cover a wider range of accelerating voltages than was used in the earlier measurements. In these latest measurements we have routinely

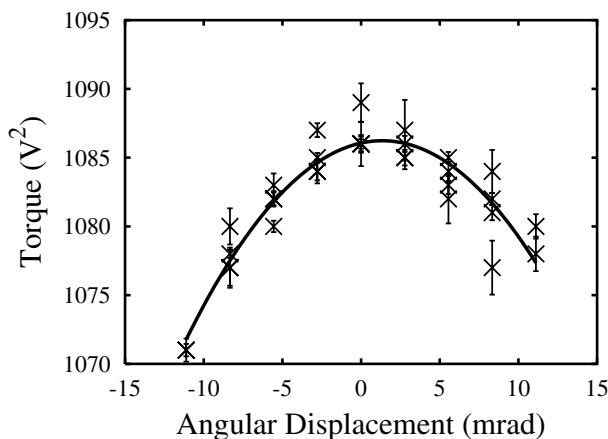


FIG. 3. A measurement of the angular variation of the torque to determine the maximum angle.

TABLE I. Standard relative uncertainties together with their effective degrees of freedom  $\nu_{\text{eff}}$  for our measurement.  $D$  is the field mass spacing,  $\phi_{\text{FM}}$  is the field mass angle at the maximum torque, and the other components are as defined in Eqs. (1) and (3).

Source	Type A		Type B	
	(parts in $10^6$ )	$\nu_{\text{eff}}$	(parts in $10^6$ )	$\nu_{\text{eff}}$
$dC/d\theta$	2	2985	19	5
$D$	2	96	5	1
$K$			12	32
$\phi_{\text{FM}}$	21	32		
$V_G$	18	1920	2	5
$V_c$	19	960		
Total	33	217	23	10

used voltages in the range 100 to 270 V. To ensure that  $dC/d\theta$  is independent of voltage, measurements of  $dC/d\theta$  have been made as low as 30 V, which is a typical value of  $V_G$ . At the low voltages, the variation of  $\Gamma_R$  seen by the apparatus as it rotates is a significant fraction of the applied torque so these results have a larger uncertainty but are still consistent with the higher voltage values.

We have also measured the temperature coefficient for  $dC/d\theta$  by deliberately changing the laboratory temperature, and the appropriate temperature coefficients have been applied to the calculations. The measured temperature correction was around 1 part in  $10^4$  per  $^\circ\text{C}$ . Over one day, the variation in temperature is less than  $0.06^\circ\text{C}$  while over a complete measurement of  $G$  it is less than  $0.2^\circ\text{C}$ .

Figure 3 shows a typical measurement of the maximum gravitationally induced torque as a function of the large mass angle. A single measurement consists of rotating the large masses around the small mass several times over a  $\pm 12$  mrad range from a nominal angle near the maximum gravitationally induced torque. The curve shown in Fig. 3 is a polynomial fitted to the experimental data. The angular displacement at the maximum torque is  $\sim 1$  mrad. This 1 mrad offset has been included in the calculation of  $K$ . However, while we can determine the angle to around 0.1 mrad in each measurement, the repeatability of the actual measurements show that the uncertainty is nearer 1 mrad.

TABLE II. Values of  $G$  measured recently using the MSL torsion balance. The standard uncertainties shown are type A only.

Large masses	$G/10^{-11} \text{ m}^3 \text{ kg}^{-1} \text{ s}^{-2}$
Cu	6.673 59(44)
Cu	6.673 98(46)
Cu	6.673 99(45)
SS	6.673 92(49)
Mean	6.673 87(22)

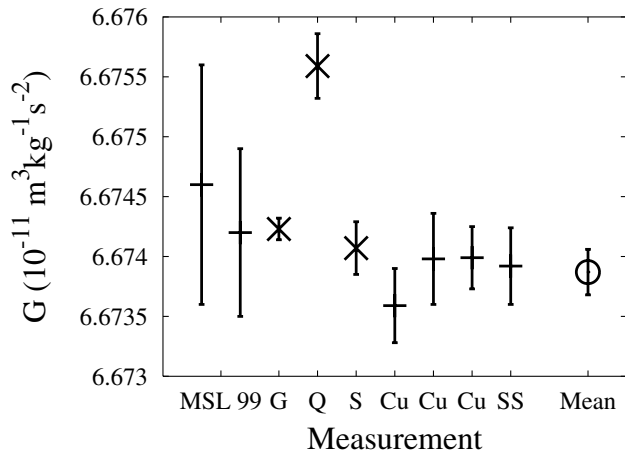


FIG. 4. Recent measurements of  $G$ . The measurements are (from left to right), the earlier MSL measurements using the compensated torsion balance, the measurements of Gundlach and Merkowitz [2], Quinn *et al.* [4], Schlamminger *et al.* [3], and the four current MSL values with their type A uncertainties. The rightmost point is the average value of the current measurements with its type A and type B uncertainties included.

Table I shows the components which make up the uncertainty in the final value of  $G$ . The values shown are for the average of the four separate measurements of  $G$ . Type B uncertainties for  $dC/d\theta$  and  $K$  are from the mass and dimensional measurements of the large and small masses. Note that although  $K$  includes the spacing of the large masses  $D$ , it is shown in the table as a separate uncertainty because it is measured many times during the measurement. For  $V_G$  type B uncertainty is due to the voltmeter calibration, and for  $D$  it is from the calibration of the length bar.

No statistically significant difference in the value of  $G$  at any of the different large mass positions was observed. This was consistent with the small variations in the measured density of the large masses. Details of these density measurements have already been reported in [5] for the stainless steel masses and in [8] for the copper masses. We have continued to rotate and move the masses to average out any small effects and also as a check on our calculation of  $K$  as the large mass spacing at the different positions changes by  $\sim 0.6$  mm.

The results of our recent measurements of  $G$  are summarized in Table II and are shown in Fig. 4 together with some of the recent measurements of  $G$ . Our new results are in good agreement with each other.

We have combined all of the recent values to obtain our best estimate of  $G$ . Our final result is  $G = 6.67387 (0.00027) \times 10^{-11} \text{ m}^3 \text{ kg}^{-1} \text{ s}^{-2}$  with a standard relative uncertainty of 41 ppm. The uncertainty consists of type A and type B components of (0.00022 and  $0.00014) \times 10^{-11} \text{ m}^3 \text{ kg}^{-1} \text{ s}^{-2}$ , respectively.

In conclusion, we believe that this current measurement of  $G$  is our best and most precise measurement and represents the best measurement which our torsion balance is capable of achieving.

The authors acknowledge the financial support received from the Marsden Fund administered by the Royal Society of New Zealand and from the Ministry of Research Science and Technology. We also acknowledge the valuable assistance of the Industrial Research mechanical workshop and the supportive assistance and advice from the staff of MSL.

\*Electronic address: t.armstrong@irl.cri.nz

- [1] P. H. Mohr and B. N. Taylor, *J. Phys. Chem. Ref. Data* **28**, 1713 (1999).
- [2] J. H. Gundlach and S. M. Merkowitz, *Phys. Rev. Lett.* **85**, 2869 (2000).
- [3] S. Schlamminger, E. Holzschuh, and W. Kundig, *Phys. Rev. Lett.* **89**, 161102 (2002).
- [4] T. J. Quinn, C. C. Speake, S. J. Richman, R. S. Davis, and A. Picard, *Phys. Rev. Lett.* **87**, 111101 (2001).
- [5] M. P. Fitzgerald and T. R. Armstrong, *IEEE Trans. Instrum. Meas.* **44**, 494 (1995).
- [6] M. P. Fitzgerald and T. R. Armstrong, *Meas. Sci. Technol.* **10**, 439 (1999).
- [7] T. R. Armstrong and M. P. Fitzgerald, in *Proceedings of the Ninth Marcel Grossmann Meeting on General Relativity*, edited by R. J. V. G. Gurzadyan and R. Ruffini (World Scientific, Singapore, 2002), p. 1779.
- [8] T. R. Armstrong and M. P. Fitzgerald, <http://141.108.24.15:8000/store/1278.pdf> (2000).
- [9] P. R. Heyl, *J. Res. Natl. Bur. Stand.* **5**, 1243 (1930).
- [10] M. P. Fitzgerald, T. R. Armstrong, R. B. Hurst, and A. C. Corney, *Metrologia* **34**, 301 (1994).